Above-threshold double ionization of helium with attosecond intense soft x-ray pulses

Kenichi L. Ishikawa*
Department of Quantum Engineering and Systems Science, Graduate School of Engineering, University of Tokyo, Hongo 7-3-1, Bunkyo-ku, Tokyo 113-8656, Japan

Katsumi Midorikawa
Laser Technology Laboratory, RIKEN (The Institute of Physical and Chemical Research), Hirosawa 2-1, Wako, Saitama 351-0198, Japan

(Received 23 March 2005; published 19 July 2005)

We theoretically study a process in which helium is doubly ionized by absorbing two soft x-ray (91.45 eV) photons from attosecond, intense high-order harmonic sources. We directly solve the time-dependent Schrödinger equation and obtain electron energy distribution in the double continuum. Our results show that between the two peaks in electron energy spectra, expected for usual sequential ionization, an additional component (anomalous component) is present. The total two photon above-threshold double ionization yield including the anomalous component is explained by sequential processes: the two electrons are ejected one by one, absorbing a single photon each. This observation rejects the intuition that nonsequential double ionization would be responsible for the anomalous component. With the help of simple semiclassical stochastic models, we discuss two possible origins of the anomalous component, namely, postionization energy exchange and second ionization during core relaxation, of which the latter is more plausible: the ionization interval is so short that the second electron is ejected while the two electrons are still exchanging energy.

DOI: 10.1103/PhysRevA.72.013407 PACS number(s): 32.80.Rm, 42.50.Hz, 42.65.Ky

I. INTRODUCTION

Double ionization, the process in which an atom ejects two electrons by absorbing a single or several photons, is classified into two categories: sequential and nonsequential. While in the former the two electrons are ejected one by one independently of each other, in the latter they are ejected simultaneously. Two mechanisms, shake-off [1] and recollision [2], underlying the nonsequential processes are known, both of which entail the correlation between the two electrons. In the shake-off mechanism [1], dominant in single-photon double ionization by an usually weak x-ray pulse, the disappearance of the first electron leads to a sudden change of the potential which the second electron feels, and it is this sudden change of the potential that "shakes the second electron off." On the other hand, in the recollision, common in the case of an intense laser pulse [3], the outer electron, ejected through multiphoton or tunneling ionization, is driven by the laser field and recollides with the core to ionize the secondary electron [2].

The recent progress in the high-order harmonic generation (HHG) technique [4–7] has enabled the development of new soft x-ray sources with two distinct characteristics. On the one hand, ultrashort pulses with a duration down to 250 attoseconds (as) can now reveal ultrafast motion of electrons inside an atom [8–10] and are applied to direct measurement of light waves [11]. On the other hand, high-power pulses produced with a phase-matching technique [12–18] can induce multiphoton ionization [19–23]; Sekikawa *et al.* [19] have characterized extreme ultraviolet (xuv) pulses (photon energy 27.9 eV) with a pulse duration of 950 as by an autocorrelation technique, based on two photon above-threshold ionization of helium, and Hasegawa *et al.* [20] have recently observed two-photon double ionization of helium by Ti:sapphire 27th harmonic pulses (photon energy 41.8 eV), and this has been applied to the autocorrelation measurement of the pulse duration of the soft x-ray pulses [24].

With such new sources at hand, then, it would be quite natural to ask ourselves how an atom is doubly ionized when ultrashort pulse length, high intensity, and short wavelength are copresent, and this has motivated several authors [25–28] to study two-photon and/or double ionization of helium by ultrashort intense xuv and soft x-ray pulses theoretically based on the time-dependent Schrödinger equation (TDSE). Helium is virtually the only multielectron atom which one can handle exactly by numerical simulation, even though lattice calculations of single-photon ionization of Li [29] have recently been reported. Parker *et al.* [25] have studied double ionization of helium by a soft x-ray pulse with a photon energy of 3.2 atomic units (a.u.) or 87 eV and a peak intensity around 10^{16} W/cm^2, and suggested the possibility of nonsequential processes. In a series of papers [26–28] Bachau and co-workers have examined energy spectra of electrons ejected through two-photon double ionization of He and Be. They have discussed the effects of electron correlation in the context of ultrashort pulses and showed that for photon energies higher than 54.4 eV, the electron left in a nonstationary bound state of He^+ has no time to relax and the two peaks corresponding to sequential ionization shift towards each other in the attosecond regime.

In this paper, we present a computational study of two-photon double ionization of helium by attosecond intense soft x-ray pulses. Specifically we consider the 13.6 nm

*Electronic address: ishiken@q.t.u-tokyo.ac.jp

wavelength, which corresponds to the 59th harmonic [8–10] of a Ti:sapphire laser (wavelength 800 nm), for which attosecond pulses have been experimentally demonstrated. For this wavelength it is also possible to obtain high intensity [15]. In particular, we examine energy spectra of the ejected electrons as a function of pulse length in detail. This provides useful information about the electron correlation under an ultrashort intense pulse. We numerically solve the time-dependent Schrödinger equation (TDSE) by close-coupling grid calculations. Our results show that between the two peaks at 37 and 67 eV due to usual sequential double ionization the electron spectra contain an extra component, which was previously attributed to nonsequential ionization [25] without detailed discussion on its mechanism. According to our analyses, however, this *anomalous component* does *not* correspond to nonsequential processes, but the two electrons are ejected one by one, absorbing a single photon each.

Furthermore, in order to explore the origin of the anomalous component, we construct simple semiclassical models to calculate electron energy spectra based on two possible mechanisms, namely, postionization energy exchange (PIEE) and second ionization during core relaxation (SICR). The latter leads to spectra which agree better with those obtained from the TDSE calculations and, thus, is more plausible as a mechanism responsible for the anomalous component as well as for the peak displacement [26–28].

The present paper is organized as follows. Section II summarizes the simulation model. In Sec. III we apply the model to the calculation of energy distribution of electrons ejected through two-photon double ionization of He by attosecond intense Ti:sapphire 59th harmonic pulses. After discussing the spectral peak shape by the usual sequential ionization, we examine how the ultrashortness of the pulse affects the spectra and, especially, discuss the origin of the anomalous component. The conclusions are given in Sec. IV. Atomic units are used throughout the paper unless otherwise stated.

II. MODEL

The interaction between He and a soft x-ray pulse is described by the two-electron TDSE,

$$i\frac{\partial\Phi(\mathbf{r}_1,\mathbf{r}_2,t)}{\partial t}=[H_0+H_I(t)]\Phi(\mathbf{r}_1,\mathbf{r}_2,t), \tag{1}$$

with the atomic Hamiltonian

$$H_0=-\frac{1}{2}\nabla_1^2-\frac{1}{2}\nabla_2^2-\frac{2}{r_1}-\frac{2}{r_2}+\frac{1}{|\mathbf{r}_1-\mathbf{r}_2|}, \tag{2}$$

and, in the length gauge,

$$H_I(t)=(z_1+z_2)E(t), \tag{3}$$

where $E(t)$ is the electric field of the pulse, assumed to be linearly polarized in the z-direction, and the subscript 1(2) refers to electron 1(2). We assume that the soft x-ray pulse has a Gaussian temporal profile:

$$E(t)=E_0\exp\left[-\frac{(2\ln 2)t^2}{T^2}\right]\cos\omega t, \tag{4}$$

where T is the full width at half-maximum (FWHM) pulse length. The frequency ω corresponds to a Ti:sapphire 59th harmonic pulse (energy 91.45 eV).

We solve Eq. (1) based on the time-dependent close-coupling method similar to those used in [25,30–32]. The two-electron wave function $\Phi(\mathbf{r}_1,\mathbf{r}_2,t)$ is expanded in coupled spherical harmonics $\Lambda^L_{l_1,l_2}(\hat{\mathbf{r}}_1,\hat{\mathbf{r}}_2)$ [33]:

$$\Phi(\mathbf{r}_1,\mathbf{r}_2,t)=\sum_L\sum_{l_1,l_2}\frac{P^L_{l_1,l_2}(r_1,r_2,t)}{r_1r_2}\Lambda^L_{l_1,l_2}(\hat{\mathbf{r}}_1,\hat{\mathbf{r}}_2), \tag{5}$$

where l_1 and l_2 are the angular momenta of the two electrons, and L is the total orbital angular momentum of the atomic system. The substitution of Eq. (5) into Eq. (1) leads to a set of time-dependent partial differential equations [30] for the radial wave functions $P^L_{l_1,l_2}(r_1,r_2,t)$, represented on a two-dimensional spatial grid. We use low-order finite difference methods with uniform mesh spacing. In order to account for the boundary condition at the origin properly, we discretize the Euler-Lagrange equations with a Lagrange-type functional [35,36],

$$\mathcal{L}=\langle\Phi|i\partial/\partial t-[H_0+H_I(t)]|\Phi\rangle, \tag{6}$$

instead of Eq. (1) itself.

The ground state of helium is found by relaxation of the TDSE in imaginary time and then time evolved by solving the TDSE in real time. We typically use a 800×800 lattice with grid spacing of 0.25 a.u., and the time step is 9.13×10^{-4} a.u. The partial waves $0\leqslant l_1,l_2,L\leqslant3$ are included, though the use of $0\leqslant l_1,l_2,L\leqslant2$ has led to virtually the same results. The contribution of each partial wave to the probability distribution $P(E_1,E_2)$ of the escaping electron energies $E_{1,2}$ can be calculated as the square of the absolute value of the projection of the two-electron radial wave function onto the product of He^{2+} continuum state radial orbitals of the two electrons [32].

III. RESULTS AND DISCUSSION

Since the photon energy (91.45 eV) is larger than the sum of the first and second ionization potential ($I_{p1}=24.6$ and $I_{p2}=54.4$ eV, respectively) of He, a single photon suffices to induce double ionization [32]. This is a linear optical effect and can be observed even with weak x-ray sources. On the other hand, with intense sources, we expect that a process where a He atom absorbs two photons and ejects two electrons takes place. In this case the atom absorbs further photons than the minimum necessary for double ionization, and thus we call it above-threshold double ionization (ATDI) [34] (the terminology "double-electron above-threshold ionization" is also found in literature [25]).

A. Electron energy distribution

In the long pulse length limit $T\to\infty$, He would be sequentially ionized, and the electron energy spectrum would have

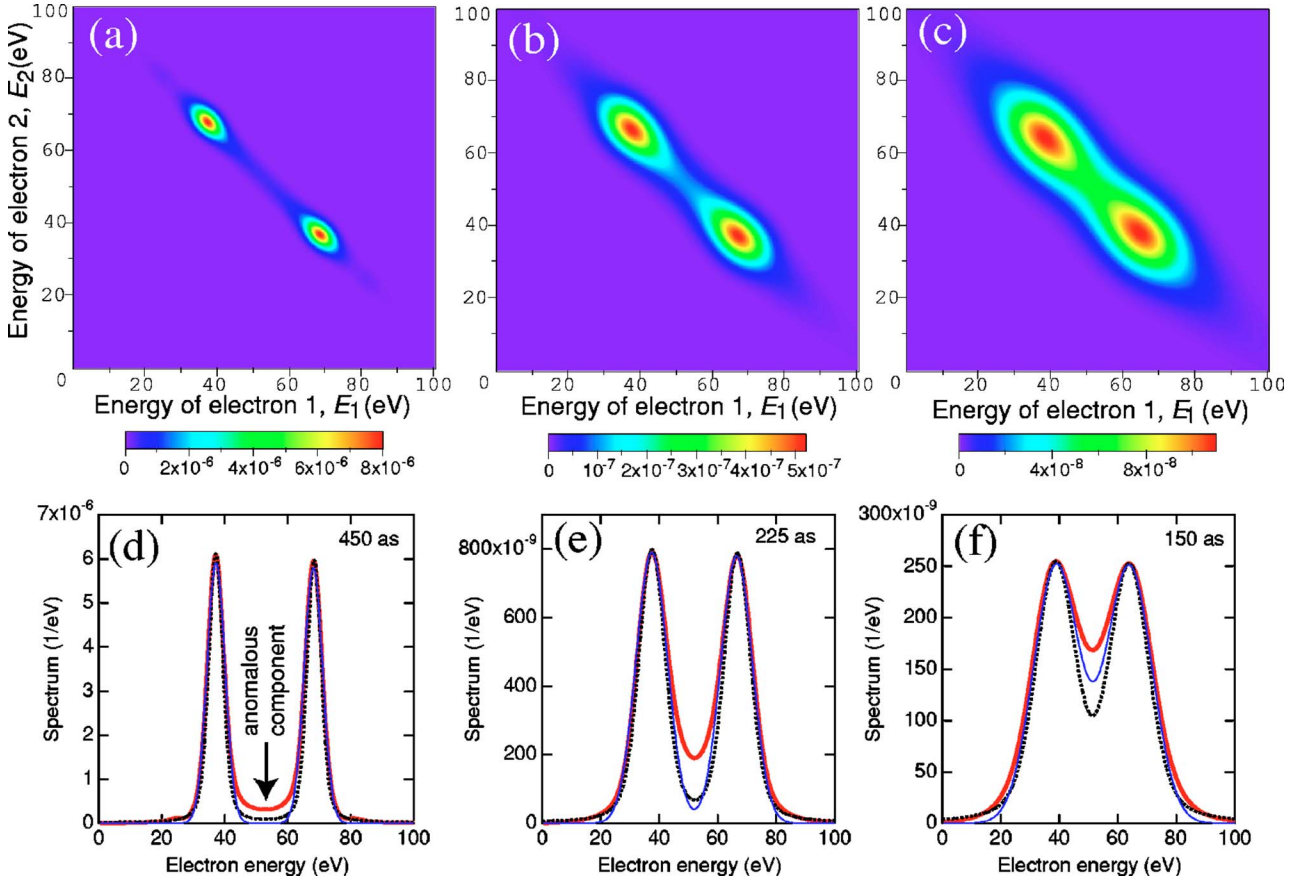

FIG. 1. (Color online) Energy distribution of the electrons ejected through two-photon double ionization by a soft x-ray pulse with a peak intensity of 10^{15} W/cm^2. (a)–(c) Probability distribution $P(E_1,E_2)$ of the energy E_1, E_2 of the two electrons for a pulse width (FWHM) of (a) 450, (b) 225, and (c) 150 as, respectively. (d)–(f) Thick solid lines: the corresponding electron energy spectra (integrated with respect to E_2), thin solid lines: the fitted curves with two Gaussian functions, and thin dotted lines: the fitted curves with the peak shape function Eq. (7).

two sharp peaks at 66.9 and 37.1 eV. Figure 1 displays the energy distribution of the electrons ejected through two-photon double ionization by an attosecond soft x-ray pulse. From this figure we can extract several effects of the ultrashort pulse duration. First, the broadened electron energy spectra have tails longer than expected for usual Gaussian profiles. In fact, when the soft x-ray pulse has a Gaussian temporal profile, the peaks for sequential two-electron double ionization do not have Gaussian shapes but the following forms (see the Appendix):

$$P_1(\Delta\omega) = P_2(\Delta\omega) \propto e^{-\Delta\omega^2/2a^2} \times \int_{-\infty}^{\infty} e^{-2a^2t^2} \left| 1 + \mathrm{erf}\left(at - \frac{i\Delta\omega}{2a} \right) \right|^2 dt, \quad (7)$$

where $a=\sqrt{2\ln 2}/T$ and $\Delta\omega$ denotes the detuning. Similarly to the Voigt profile, this profile tends to the Gaussian one at the center ($\Delta\omega=0$) and decreases as $1/\Delta\omega^2$ for a large value of $|\Delta\omega|$, which leads to the long tails seen in Figs. 1(d)–1(f).

We note that Fig. 1(d) contains small maxima around 25 and 80 eV. These correspond to a process in which the first single photon ionization leaves the He^+ ion in the $2s$ or $2p$ excited states, situated 40.8 eV above the ground state and 13.6 eV below the second ionization threshold:

$$\mathrm{He} + h\nu \rightarrow \mathrm{He}^+(2s,2p) + e^-. \quad (8)$$

In this case, the first and second ejected electrons have an energy of 26 and 78 eV, respectively, which explains the small maxima in Fig. 1(d). Although not possible to identify in Fig. 1 there exist, in principle, processes in which the first ionization leaves the He^+ ion in other excited states, which are subsequently ionized to He^{2+}:

$$\mathrm{He} + h\nu \rightarrow \mathrm{He}^+(nl) + e^-, \quad (9)$$

$$\mathrm{He}^+(nl) + h\nu \rightarrow \mathrm{He}^{2+} + e^-, \quad (10)$$

where n and l denote the principal and azimuthal quantum number, respectively. Table I summarizes the cross section $\sigma_1(nl)$ of reaction Eq. (9) and $\sigma_2(nl)$ of reaction Eq. (10) for the ground state and several excited levels of He^+. In the rightmost column listed are $\sigma_1(nl)\sigma_2(nl)/\sigma_1(1s)\sigma_2(1s)$, i.e., the relative height of each contribution to the electron energy spectrum resulting from the sequential ionization. The relative contribution rapidly decreases with increasing principal

TABLE I. The values of cross section $\sigma_1(nl)$ of reaction Eq. (9) and $\sigma_2(nl)$ of reaction Eq. (10) for several levels of He^+. The former is obtained from the yield of $He^+(nl)$ in the present TDSE simulations, and the latter with the hydrogenic wave functions. The rightmost column is the relative height of each contribution to the electron energy spectrum resulting from the sequential ionization.

nl	$\sigma_1(nl)$	$\sigma_2(nl)$	$\frac{\sigma_1(nl)\sigma_2(nl)}{\sigma_1(1s)\sigma_2(1s)}$
$1s$	4.9×10^{-19}	3.8×10^{-19}	1
$2s$	1.8×10^{-20}	3.8×10^{-20}	3.7×10^{-3}
$2p$	1.3×10^{-20}	7.4×10^{-21}	5.2×10^{-4}
$3s$	2.2×10^{-21}	7.8×10^{-21}	9.2×10^{-5}
$3p$	2.0×10^{-21}	2.4×10^{-21}	2.6×10^{-5}

quantum number. Thus the peaks associated with the states with $n\geqslant 3$ are invisible in Figs. 1(d)–1(f).

The dotted lines in Figs. 1(d)–1(f) represent the fitting with two functions of the form Eq. (7). By comparison between the solid and dotted lines we can see that a component other than the usual sequential double ionization is present. At the 450 as pulse length [Figs. 1(a) and 1(d)], for example, between the two peaks at 67 and 37 eV (usual sequential ATDI), we can see a small but clear signature of the presence of a third component, which cannot be reproduced by the fitting. We call this the *anomalous component* hereafter, since this portion of the spectrum cannot be explained by the usual sequential ATDI. As the pulse length decreases [Figs. 1(b), 1(c), 1(e), and 1(f)], the peaks for sequential ATDI become broader. The anomalous component is, however, present. As can be seen from Figs. 1(a)–1(c), the electron energy is distributed along the line $E_1+E_2=104$ eV. Thus, in the anomalous component, the two electrons share the two photon energy, which evidently indicates electron correlation. We have repeated simulations by varying the peak intensity I_0 between 10^{14} and 10^{16} W/cm^2 and confirmed that the results scale as I_0^2, appropriate for two-photon processes, which becomes prominent at high intensity.

B. Anomalous component

Let us discuss the origin of the anomalous component in this section. At a glance, we would be tempted to assign the anomalous component to a nonsequential process in which the two electrons absorb two photons at the same time and share energy, as did the authors of Ref. [25], which reported similar results. However, it turns out to be incorrect by the following analysis. The yield of sequential ATDI is given by

$$\int_{-\infty}^{\infty} dt\sigma_1\frac{I(t)}{\hbar\omega}\int_{t}^{\infty} dt'\sigma_2\frac{I(t')}{\hbar\omega} = \sigma_1\sigma_2\frac{\pi}{8\ln 2}\left(\frac{I_0}{\hbar\omega}\right)^2 T^2, \tag{11}$$

and scales as T^2, where $I(t)$ is the soft x-ray temporal intensity profile, and σ_1 (σ_2) is the single ionization cross section of He (He^+). On the other hand, the yield of nonsequential ATDI, if any, would be given by

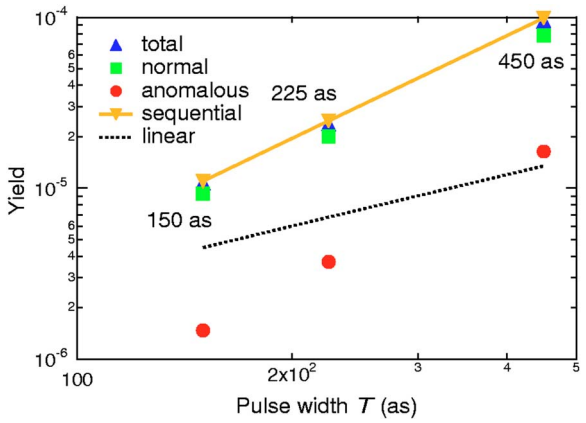

FIG. 2. (Color online) Electron yield by usual sequential double ionization (green squares) and anomalous double ionization (red circles) as a function of pulse width T. Blue triangles are the total yield. Yellow solid line is calculated from Eq. (11) with $\sigma_1=4.87\times10^{-19}$ cm^2 and $\sigma_2=3.80\times10^{-19}$ cm^2, and scale as T^2. A function scaling linearly with T should be parallel to the dotted line.

$$\int_{-\infty}^{\infty} dt\sigma_{NS}\left(\frac{I(t)}{\hbar\omega}\right)^2 = \sigma_{NS}\sqrt{\frac{\pi}{8\ln 2}}\left(\frac{I_0}{\hbar\omega}\right)^2 T, \tag{12}$$

and thus would scale as T, where σ_{NS} is the corresponding cross section. Although it is not easy to separate unambiguously the usual sequential ATDI components and the anomalous component in Fig. 1, we have tried to do it by attributing the dotted lines in Figs. 1(d)–1(f) to the normal components and the difference between the solid and dotted lines to the anomalous components. Thus obtained normal and anomalous yields as a function of T are shown in Fig. 2. Each of the normal and anomalous components is seen to scale approximately as T^2, and the total yield scales nearly exactly as T^2. Moreover, the total yield agrees well with the one calculated from Eq. (11) by use of the values of $\sigma_1(1s)$ and $\sigma_2(1s)$ listed in Table I. This observation clearly indicates that the contribution of nonsequential ATDI, if any, is negligible at most and that the entire ATDI consists of sequential processes.

Then how do we interpret the presence of the anomalous component? If we assume that the first and second ionization takes place independently of each other, the ionization interval Δt is distributed according to the following probability distribution:

$$P(\Delta t) = \frac{2\sqrt{2\ln 2}}{T\sqrt{\pi}}e^{-2\ln 2\Delta t^2/T^2}. \tag{13}$$

The mean interval is calculated to be $T/\sqrt{2\pi\ln 2}$; specifically 72, 108, and 216 as for the 150, 225, and 450 as pulse length, respectively. Based on the ultrashortness of the ionization interval, we may consider two candidates for the mechanism responsible for the anomalous component as follows.

1. Postionization energy exchange (PIEE): during 72 as, for example, the first electron can escape only 6.6 times Bohr radius. Hence when the second electron is ejected, the first

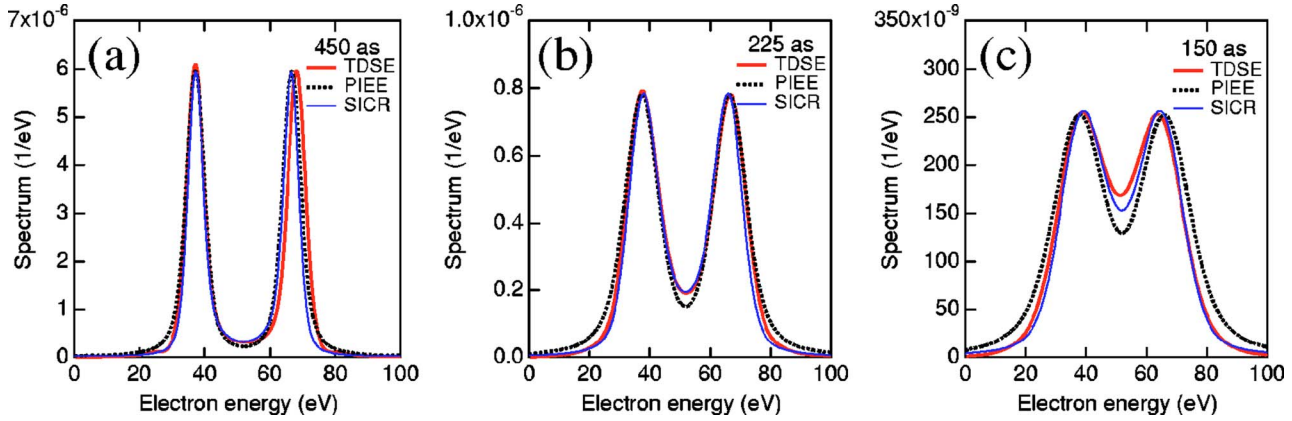

FIG. 3. (Color online) Electron energy spectra calculated with the TDSE calculations (thick solid lines), PIEE (dotted lines), and SICR (thin solid lines) models. The soft x-ray pulses are assumed to be of a Gaussian temporal profile with a FWHM duration of (a) 450, (b) 225, and (c) 150 as.

one is still very close to the nucleus with significant probability. It is, therefore, expected that the distance between the two escaping electrons is so short that they can exchange energy through Coulomb interaction and that this might manifest itself as the anomalous component.

2. Second ionization during core relaxation (SICR) [26–28]: since the two electrons in the ground state He atom are equivalent, at the very moment of the first ionization the remaining He^+ ion cannot be in the ground state but in a nonstationary state whose average energy would be $-(I_{p1}+I_{p2})/2=-39.5$ eV [27]. The nonstationary He^+ is expected to relax to the ground state with a correlation time τ of ca. 22 as, related to $I_{p2}-I_{p1}$. The anomalous component might correspond to the situation where the second electron is emitted within this core relaxation time.

In order to explore which of the two is responsible for the emergence of the anomalous component, we have constructed simple semiclassical models in which ionization events are described stochastically. The ionization interval Δt is chosen randomly according to the distribution in Eq. (13). For the verification of the PIEE picture, we calculate the distance of the first electron at the instant of the second ionization by assuming classical motion with an energy of 66.9 eV under the Coulomb force of a point charge $+e$ at the origin. The second electron is put near the origin with an initial velocity in such a way that the system of the immobile nucleus and the two escaping electrons has a total energy of 104 eV. The initial direction of each p electron is randomly distributed as $\cos^2\theta$, where θ is the angle from the z axis and the subsequent motion is calculated by integrating the classical equation of motion under the Coulomb force of the nucleus and the mutual Coulomb interaction using the fourth-order Runge-Kutta method with adaptive step-size control. The influence of the soft x-ray field on the electron motion is neglected. For the verification of the SICR picture, on the other hand, the ionization potentials are assumed to depend on Δt as follows:

$$I_{p1}(\Delta t) = 24.6 + 14.9e^{-t/\tau}\,(\mathrm{eV}), \tag{14}$$

$$I_{p2}(\Delta t) = 54.4 - 14.9e^{-t/\tau}\,(\mathrm{eV}). \tag{15}$$

We calculate the energy of ejected electrons from the values of I_{p1} and I_{p2} obtained by these equations with randomly sampled Δt.

Typically 100,000 runs are carried out for each pulse length, and the distribution of the final electron kinetic energy is folded with the peak shape function Eq. (7), to mimic the effect of the Heisenberg uncertainty principle. Thus obtained spectra are compared with the results of the TDSE simulations in Fig. 3. One of the qualitative differences between the two semiclassical models is that in the PIEE model the energy exchange can lead to the acceleration of the first electron and the deceleration of the second, populating also the region *outside* the two peaks in the electron energy spectrum. On the other hand, the SICR can populate only the region *between* the peaks. In fact, in Fig. 3, we can see that the PIEE model overestimates the spectrum outside the two peaks. Furthermore, the component between the peaks is better reproduced by the SICR model. Considering its simplicity, the quantitative agreement between the TDSE calculation and the SICR model is surprising, though not perfect. This supports the SICR rather than the PIEE as the origin of the anomalous component as well as our view that the entire ATDI is essentially a sequential process.

Laulan and Bachau [26–28] have reported that the distance between the two peaks decreases for shorter pulse duration. This phonomenon can also be confirmed by our TDSE and SICR simulation as shown in Fig. 4, while the distance between the peaks is nearly independent of pulse width in the case of the PIEE model; a slight decrease for shorter pulse width for PIEE in Fig. 4 is due to overlap of the tail of one peak to the other. This again supports the idea that the SICR mechanism plays an important role in the ATDI of He by an ultrashort intense soft x-ray pulse.

It should, however, be noted that the anomalous component is the most visible at a pulse length of 450 as and that the PIEE also reproduces the spectrum between the two peaks quite well in Fig. 3(a). Thus the PIEE may not be excluded conclusively as an additional origin of the anoma-

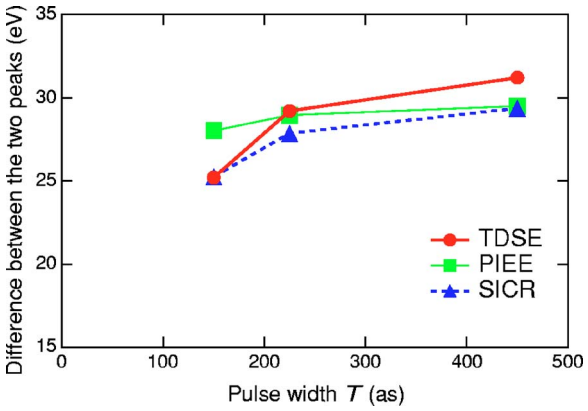

FIG. 4. (Color online) Difference between the two peaks in the electron energy spectra calculated with the TDSE calculations (thick solid lines), PIEE (thin solid lines), and SICR (dashed lines) models, as a function of pulse width T.

lous component. This point as well as the explanation of the quantitative discrepancy between the TDSE simulation and the SICR model in Fig. 4 would need further investigation.

IV. CONCLUSIONS

Using numerical simulations based on the two-electron time-dependent Schrödinger equation, we have investigated the above-threshold two-photon double ionization of He by an attosecond, intense soft x-ray pulse, specifically a Ti:sapphire 59th harmonic pulse. The one-electron energy spectrum consists of two major peaks around 37 and 67 eV corresponding to usual sequential ionization and the anomalous component between them. For an incident pulse of a Gaussian temporal profile, the major peaks have quadratically decreasing long tails. Although the peak shape is common for any pulse duration apart from the width, the long tails would not become visible until the use of ultrashort pulses.

The two-photon double ionization yield scales as the square of pulse width, which indicates that the entire electron energy spectrum including the anomalous component is the outcome of sequential ionization and that the contribution of nonsequential processes is virtually absent. The major origin of the anomalous component is second ionization during core relaxation, i.e., events where the second electron is ejected by absorbing a single photon, while a nonstationary state of He^+ is relaxing to the ground state and the two electrons are still exchanging energy, though postionization energy exchange may also be present. Hence, in either case, the anomalous component is a remarkable manifestation of electron correlation in the attosecond pulse regime, alongside the peak displacement [26–28].

It is noteworthy that electron correlation can play a significant role even in a sequential ionization process. The ionization of the second electron itself can proceed by photon absorption, whether electron correlation may be present or not. In this sense, the double ionization is *not* nonsequential. This is in striking contrast to shake-off [1] and recollision [2], in which energy exchange is indispensable for the ejection of the inner electron. High-intensity alone is not sufficient for the anomalous ATDI to be of comparable prominence with the usual sequential ATDI, but attosecond pulses are also necessary. Thus the combination of the ultrashortness, high intensity, and short wavelength furnished by the state-of-the-art soft x-ray sources based on HHG will serve as a unique tool to study inneratom electron correlation dynamics under a strong field. The anomalous ATDI, present also in more complex atoms [28] in principle, will be an attractive example to be explored.

ACKNOWLEDGMENTS

This work has been partially supported by Ministry of Education, Culture, Sports, Science and Technology of Japan Grants No. 15035203 and No. 15740252, and also by a grant from Research Foundation for Opto-Science and Technology.

APPENDIX: SHAPE OF SEQUENTIAL TWO-PHOTON DOUBLE IONIZATION PEAKS

Let us consider a three-level system whose lowest (energy ω_1), intermediate (ω_2), and highest (ω_3) levels corresponds to the ground-state He atom, $He^+ + e^-$, and $He^{2+} + 2e^-$, respectively. The transition frequency $\omega_{21} = \omega_2 - \omega_1$ and $\omega_{32} = \omega_3 - \omega_2$ are assumed to be close to ω. We write the Schrödinger equation and the wave function of this system as

$$i\frac{\partial}{\partial t}\Phi(t) = [H_0 + \mu V(t)\cos\omega t]\Phi(t), \tag{A1}$$

where μ denotes the dipole operator and $V(t)$ the pulse envelope, and

$$\Phi(t) = \sum_{i=1}^{3} C_i(t)\Phi_i \exp(-i\omega t), \tag{A2}$$

where $C_i(t)$ $(i=1,\ldots,3)$ denotes the time-dependent expansion coefficient, and Φ_i $(i=1,\ldots,3)$ the time-independent wave function of level i. Substituting Eq. (A2) into Eq. (A1), making the rotating-wave approximation, and assuming $|C_3| \ll |C_2| \ll |C_1| \approx 1$, we obtain

$$C_2(t) \propto \int_{-\infty}^{t} dt' V(t') e^{i(\omega_{21}-\omega)t'} \tag{A3}$$

and

$$C_3(t) \propto \int_{-\infty}^{t} dt' V(t') e^{i(\omega_{32}-\omega)t'} \int_{-\infty}^{t'} dt'' V(t'') e^{i(\omega_{21}-\omega)t''}. \tag{A4}$$

Especially, the final amplitude $C(\infty)$ of level 3 after the pulse is written as

$$C_3(\infty) \propto \int_{-\infty}^{\infty} dt V(t) e^{i(\omega_{32}-\omega)t} \int_{-\infty}^{t} dt' V(t') e^{i(\omega_{21}-\omega)t'} \tag{A5}$$

$$= \int_{-\infty}^{\infty} dt V(t) e^{i(\omega_{21}-\omega)t} \int_{t}^{\infty} dt' V(t') e^{i(\omega_{32}-\omega)t'}. \quad \text{(A6)}$$

Noting that $\omega_{21}-I_{p1}$ corresponds to the first ionization peak at 67 eV and $\omega_{32}-I_{p2}$ the second peak at 37 eV, the shape of the first and second peak are given by

$$P_1(\Delta\omega_{21}) \propto \int_{-\infty}^{\infty} |C_3(\infty)|^2 d\omega_{32} \quad \text{(A7)}$$

and

$$P_2(\Delta\omega_{32}) \propto \int_{-\infty}^{\infty} |C_3(\infty)|^2 d\omega_{21}, \quad \text{(A8)}$$

respectively, where $\Delta\omega_{21}=\omega_{21}-\omega$ and $\Delta\omega_{32}=\omega_{32}-\omega$. From Eqs. (A5) and (A6), $C_3(\infty)$ can be viewed as the Fourier transform of

$$V(t) \int_{-\infty}^{t} dt' V(t') e^{i\Delta\omega_{21}t'}, \quad \text{(A9)}$$

with respect to the detuning $\Delta\omega_{32}$, or that of

$$V(t) \int_{t}^{\infty} dt' V(t') e^{i\Delta\omega_{32}t'}, \quad \text{(A10)}$$

with respect to $\Delta\omega_{21}$. Then, by use of Parseval's formula, after some algebra, we can rewrite the spectral shapes $P_{1,2}(\Delta\omega)$ in Eqs. (A7) and (A8) as

$$P_1(\Delta\omega) \propto \int_{-\infty}^{\infty} \left| V(t) \int_{-\infty}^{t} dt' V(t') e^{i\Delta\omega t'} \right|^2 dt \quad \text{(A11)}$$

and

$$P_2(\Delta\omega) \propto \int_{-\infty}^{\infty} \left| V(-t) \int_{-\infty}^{t} dt' V(-t') e^{i\Delta\omega t'} \right|^2 dt. \quad \text{(A12)}$$

It should be noted that $P_1(\Delta\omega)=P_2(\Delta\omega)$ for a symmetric pulse envelope, i.e., $V(t)=V(-t)$. Specifically, for a Gaussian temporal profile, $V(t) \propto e^{-2\ln 2 t^2/T^2}$, we finally obtain

$$P_1(\Delta\omega) = P_2(\Delta\omega) \propto e^{-\Delta\omega^2/2a^2} \times \int_{-\infty}^{\infty} e^{-2a^2t^2} \left| 1 + \mathrm{erf}\left(at - \frac{i\Delta\omega}{2a} \right) \right|^2 dt, \quad \text{(A13)}$$

where $a=\sqrt{2\ln 2}/T$.

[1] T. Pattard, T. Schneider, and J. M. Rost, J. Phys. B **36**, L189 (2003).
[2] P. B. Corkum, Phys. Rev. Lett. **71**, 1994 (1993).
[3] B. Walker, B. Sheehy, L. F. DiMauro, P. Agostini, K. J. Schafer, and K. C. Kulander, Phys. Rev. Lett. **73**, 1227 (1994).
[4] A. McPherson, G. Gibson, H. Jara, U. Johann, T. S. Luk, I. A. McInstyre, K. Boyer, and C. K. Rhodes, J. Opt. Soc. Am. B **4**, 595 (1987).
[5] M. Ferray, A. L'Huillier, X. F. Li, L. A. Lompré, G. Mainfray, and C. Manus, J. Phys. B **21**, L31 (1988).
[6] A. L'Huillier and Ph. Balcou, Phys. Rev. Lett. **70**, 774 (1993).
[7] J. J. Macklin, J. D. Kmetec, and C. L. Gordon III, Phys. Rev. Lett. **70**, 766 (1993).
[8] M. Drescher, M. Hentschel, R. Kienberger, M. Uiberacker, V. Yakovlev, A. Scrinzi, Th. Westerwalbesloh, U. Kleineberg, U. Heinzmann, and F. Krausz, Nature (London) **419**, 803 (2002).
[9] A. Baltuska, Th. Udem, M. Uiberacker, M. Hentschel, E. Goulielmakis, Ch. Gohle, R. Holzwarth, V. S. Yakovlev, A. Scrinzi, T. W. Hänsch, and F. Krausz, Nature (London) **421**, 611 (2003).
[10] R. Kienberger, E. Goulielmakis, M. Uiberacker, A. Baltuska, V. Yakovlev, F. Bammer, A. Scrinzi, Th. Westerwalbesloh, U. Kleineberg, U. Heinzmann, M. Drescher, and F. Krausz, Nature (London) **427**, 817 (2004).
[11] E. Goulielmakis, M. Uiberacker, R. Kienberger, A. Baltuska, V. Yakovlev, A. Scrinzi, Th. Westerwalbesloh, U. Kleineberg, U. Heinzmann, M. Drescher, and F. Krausz, Science **305**, 1267 (2004).
[12] Y. Tamaki, J. Itatani, Y. Nagata, M. Obara, and K. Midorikawa, Phys. Rev. Lett. **82**, 1422 (1999).
[13] E. Takahashi, Y. Nabekawa, T. Otsuka, M. Obara, and K. Midorikawa, Phys. Rev. A **66**, 021802(R) (2002).
[14] E. Takahashi, Y. Nabekawa, and K. Midorikawa, Opt. Lett. **27**, 1920 (2002).
[15] E. J. Takahashi, Y. Nabekawa, and K. Midorikawa, Appl. Phys. Lett. **84**, 4 (2004).
[16] J.-F. Hergott, M. Kovacev, H. Merdji, C. Hubert, Y. Mairesse, E. Jean, P. Breger, P. Agostini, B. Carré, and P. Salierès, Phys. Rev. A **66**, 021801(R) (2002).
[17] D. Yoshitomi, T. Shimizu, T. Sekikawa, and S. Watanabe, Opt. Lett. **27**, 2170 (2002).
[18] H. Mashiko, A. Suda, and K. Midorikawa, Opt. Lett. **29**, 1927 (2004).
[19] T. Sekikawa, A. Kosuge, T. Kanai, and S. Watanabe, Nature (London) **432**, 605 (2004).
[20] H. Hasegawa, E. J. Takahashi, Y. Nabekawa, K. L. Ishikawa, and K. Midorikawa, Phys. Rev. A **71**, 023407 (2005).
[21] K. Ishikawa, Phys. Rev. Lett. **91**, 043002 (2003).
[22] K. L. Ishikawa, Appl. Phys. B: Lasers Opt. **78**, 855 (2004).
[23] K. L. Ishikawa, Phys. Rev. A **70**, 013412 (2004).
[24] Y. Nabekawa, H. Hasegawa, E. J. Takahashi, and K. Midorikawa, Phys. Rev. Lett. **94**, 043001 (2005).
[25] J. S. Parker, L. R. Moore, K. J. Meharg, D. Dundas, and K. T. Taylor, J. Phys. B **34**, L69 (2001).
[26] S. Laulan and H. Bachau, Phys. Rev. A **68**, 013409 (2003).
[27] B. Piraux, J. Bauer, S. Laulan, and H. Bachau, Eur. Phys. J. D **26**, 7 (2003).
[28] S. Laulan and H. Bachau, Phys. Rev. A **69**, 033408 (2004).

[29] J. Colgan, M. S. Pindzola, and F. Robicheaux, Phys. Rev. Lett. **93**, 053201 (2004).
[30] M. S. Pindzola and F. Robicheaux, Phys. Rev. A **57**, 318 (1998).
[31] M. S. Pindzola and F. Robicheaux, J. Phys. B **31**, L823 (1998).
[32] J. Colgan, M. S. Pindzola, and F. Robicheaux, J. Phys. B **34**, L457 (2001).
[33] S. P. Goldman and T. Glickman, Phys. Rev. A **55**, 1772 (1997).
[34] A. Becker and F. H. M. Faisal, Phys. Rev. A **50**, 3256 (1994).
[35] K. C. Kulander, K. J. Schafer, and J. L. Krause, in *Atoms in Intense Laser Fields*, edited by M. Gavrila, (Academic, New York, 1992), pp. 247–300.
[36] S. E. Koonin, K. T. R. Davies, V. Maruhn-Rezwani, H. Feldmeier, S. J. Krieger, and J. W. Negele, Phys. Rev. C **15**, 1359 (1977).